IL33 mediates cardiomyopathy after acute kidney injury by directly signaling to cardiomyocytes

Nans FLORENS,[1] Allen J. YORK,[1] Rajesh K. KASAM,[1] Valeria RUDMAN-MELNICK,[2] Scott N. BLAIR,[1] Vikram PRASAD,[1] Jeffery D. MOLKENTIN.[1]

1. Department of Pediatrics, University of Cincinnati, Cincinnati Children's Hospital Medical Center, Cincinnati, OH, USA.
2. Division of Nephrology and Hypertension, Cincinnati Children's Medical Center, Cincinnati, Ohio

Abstract

Background and Aims: Acute kidney injury (AKI) is a major cardiovascular risk factor, regardless of the severity or the origin of the AKI. However, few direct molecular mechanisms have been identified that show how AKI leads to cardiac disease and maladaptation. The aims of this project are to assess the role of IL33 in remote cardiac damage after AKI.

Method: AKI was induced in mice by ischemia-reperfusion injury of both right and left kidneys by 30 min of reversible artery occlusion in WT mice, IL33 null mice and mice in which the IL33-receptor was deleted in cardiomyocytes from the heart. We also generated AAV9 carrying the IL33 cDNA (AAV-IL33) or an empty vector (AAV-EV) under a CMV promoter and injected 1012 viral particles intrathoracically in 6 to 9 days-old pups. Mice containing an insertion of a MerCreMer cDNA driven by the alpha-MHC (αMHCMCM, cardiomyocyte specific) 5 kb promoter (transgene) were crossed with a Il1rl1-loxP(fl)-targeted mouse (Il1rl1fl/fl, IL33-receptor) and recombination was obtained by intraperitoneal tamoxifen injections. Echocardiography was performed either at baseline or 28 days after AKI surgery. Hearts were analyzed for fibrosis (picrosirius red staining), cardiomyocyte area measurement, capillary content and myocardial ischemia with 2-nitroimidazole (EF5).

Results: AKI induced cardiac dysfunction after 28 days, measured with echocardiography (mean ejection fraction (EF): 58 in shams and 46% with AKI, p<0.05). We observed increased fibrosis area in hearts from WT mice after AKI compared to Sham (2.3 vs 4.5% area, p<0.05) and increased cardiomyocyte surface areas indicative of hypertrophy (333 vs 597 µm2 in Sham and AKI respectively, p<0.05). Compared to Sham, WT AKI mice exhibited a capillary rarefaction (CD31 staining) along with increased myocardial EF5 staining, suggesting ongoing ischemia. However, cardiac function and architecture were preserved after 28 days of AKI in IL33 gene deleted mice. Moreover, WT mice injected with AAV9-IL33 showed impaired cardiac function compared to AAV9-EV injected ones after 8 weeks (EF 58 vs 42%, p<0.05). After AKI, targeted deletion of the IL33-receptor gene in cardiomyocytes (αMHCMCM Il1rl1fl/fl mice), preserved cardiac function and architecture with no significant increase in fibrosis, hypertrophy and no significant capillary rarefaction compared to Sham-operated mice (αMHCMCM only mice).

Conclusion: IL33 is a paracrine agent secreted during renal inflammation that then has a direct toxic effect on the heart. Our observations are in contrast to some previous reports in the literature where IL33 was suggested to function as a cardioprotective factor.

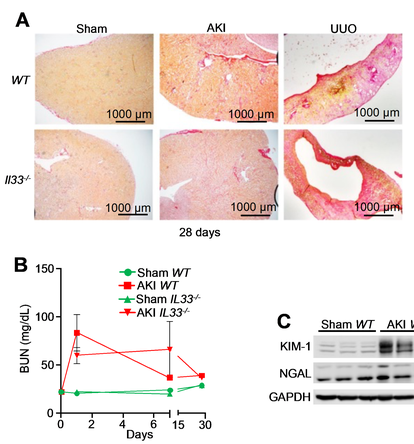

Supplemental Figure 1. Characteristics of acute renal injury in WT and *Il33*$^{-/-}$ mice after AKI. (C) Representative picrosirius red staining of kidney histological sections from mice after 28 days of sham, AKI and UUO surgeries in either WT or *Il33*$^{-/-}$ mice. Scale bar, 1000 µm. **(B)** Blood urea nitrogen (BUN) levels after sham or AKI surgery in either WT or *Il33*$^{-/-}$ mice. BUN levels were assayed at baseline (0), or after 24 h, 7 d and 28 d after surgery. No statistical differences were found between either Sham WT and *Il33*$^{-/-}$ mice or AKI WT and *Il33*$^{-/-}$ mice. Data are expressed as mean ± SEM (standard error to the mean). N=3 to 9 per group. **(C)** Western blotting for KIM-1 and NGAL (lipocalin-2) protein levels in kidney lysates from mice 24 h after sham or AKI in WT or *Il33*$^{-/-}$ mice. Glyceraldehyde 3-phophate dehydrogenase (GAPDH) was used as a loading control.

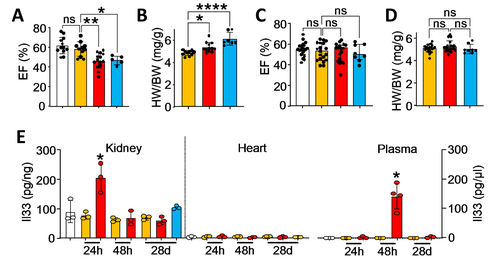

Figure 1. Acute kidney injury (AKI) drives cardiac remodeling and dysfunction in WT but not Il33 deficient mice. (A) Echocardiography measured left ventricular ejection (EF) fraction at baseline and after 4 wks of sham, AKI or UUO surgeries in WT mice. Data are presented as mean ± SD (standard deviation). N=5 to 14 per group. (B) Heart weight to body weight (HW/BW) ratio after 4 wks of either sham, AKI or UUO surgeries in WT mice. Data are presented as mean ± SD (standard deviation). N=7 to 14 per group. (C) Echocardiography measured left ventricular ejection fraction at baseline and after 4 wks of sham, AKI or UUO surgeries in Il33-/- mice. Data are presented as mean ± SD (standard deviation). N=8 to 19 per group. (D) Heart weight to body weight ratio after 4 wks of either sham, AKI or UUO surgeries in Il33-/- mice. n=8 to 19 per group. (E) Il33 protein levels in kidney lysates and heart lysates (pg/ng of tissue) or plasma (in pg/µL) in WT mice assayed by ELISA assay. Data are presented as Median ± IR (interquartile range). n=3 to 4 per group. * p<0.05, **p<0.01, ***p<0.001, ****p<0.0001, ns, p>0.05.

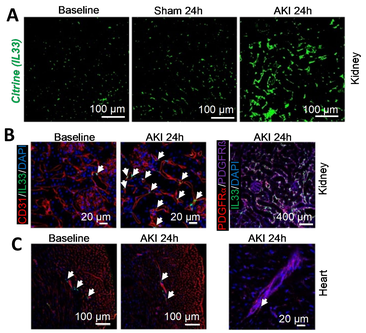

Figure 2. With AKI IL33 is expressed in endothelial and mesenchymal cells in the kidneys, but very rarely in cells of the heart. (A) Representative kidney histological sections for citrine reporter expression at baseline and 1 day after sham or AKI surgery. Scalebar 100 µm. (B) Representative staining of kidneys at baseline and after 1 day of AKI in higher magnification histological sections, which shows expression in endothelial cells (CD31 positive) and mesenchymal cells that are PDGFRα PDGFRβ positive (white arrows). Scalebars are shown in the panels. (C) Representative cardiac histological sections showing expression of the citrine reporter at baseline or after either sham or AKI surgeries for 24 hrs. Here the citrine marker was limited to rare peri-vascular fibroblasts that were PDGFRα positive but PDGFRβ negative. Scalebars are shown in the panels.

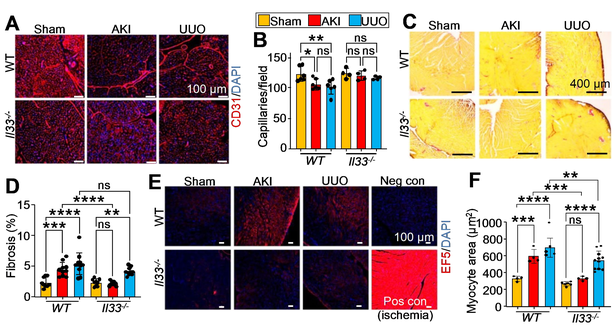

Figure 3. AKI induces cardiac capillary rarefaction, ischemia and fibrosis in WT but not in Il33-/- mice. (A) Representative histological CD31 stained heart sections and images taken 4 wks after sham, AKI and UUO surgeries in either WT or Il33-/- mice. Scale bar, 100 µm. (B) Quantification of the absolute number of capillaries per microscopic field after 4 wks of sham, AKI and UUO surgeries in either WT or Il33-/- mice. n=4 to 6 per group, with images from 5 sections analyzed per heart. Data are presented as mean ± SD (standard deviation). The legend corresponds to all data in the figure. (D) Representative picrosirius red staining of cardiac histological sections from mice after 4 wks of sham, AKI and UUO surgeries of either WT or Il33-/- genotypes. Scale bar, 400 µm. (E) Quantitative evaluation of cardiac fibrosis from the type of histological data shown in C, but across 7 to 10 mice per group, with images from at least 5 sections analyzed per heart. Data are presented as mean ± SD. (E) Representative EF5 staining of cardiac histological sections after 4 wks of sham, AKI and UUO surgeries in either WT or Il33-/- mice. Positive and negative controls are shown. Scale bar, 100 µm. (F) Myocyte cross-sectional area (µm2) from cardiac histological sections was assessed with ImageJ software after WGA-staining to outline the cells. Data were collected from hearts of mice after 4 wks of sham, AKI and UUO surgeries in either WT or Il33-/- mice. N= 4 to 11 per group and 3 sections per heart. Data are presented as mean ± SD. * p<0.05, **p<0.01, ***p<0.001, ****p<0.0001, ns, p>0.05.

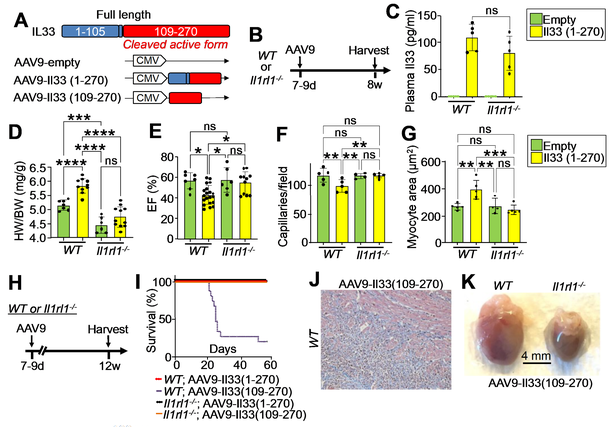

Figure 4. Il33 overexpression with AAV9 leads to cardiac remodeling but not in Il1rl1-/- mice. (A) Schematic representation of Il33 protein (top) and the different constructs to express either full-length Il33 (270 amino acids) or the activated and cleaved from (red), driven by the CMV promoter. (B) Experimental timing of AAV9 injection in either WT or Il33-receptor deficient (Il1rl1-/-) mice. (C) Il33 plasma levels were assayed by ELISA from WT and Il1rl1-/- mice injected with AAV9-empty vector or full-length Il33. Il33 was not detected in the plasma of AAV9-empty vector injected mice. (D) Heart weight to body weight (HW/BW) ratio in AAV9-Il33(1-270) compared to empty vector in both WT and Il1rl1-/- mice N=7 to 11 per group. (E) Echocardiography measured ejection fraction (EF) of the left ventricle in AAV9-Il33 (1-270) compared to empty vector in both WT and Il1rl1-/- mice. N=7 to 20 per group. (F) Quantification of capillaries per 400X microscopic field in cardiac histological sections from hearts of mice injected with AAV9-Il33(1-270) compared to AAV9-empty vector in both WT and Il1rl1-/- genotypes. N=4 to 5 per group. (G) Myocyte cross-sectional area (µm2) assessed with ImageJ on WGA-stained cardiac histological slides obtained in mice previously injected with AAV9-Il33(1-270) compared to AAV9-empty vector in both WT and Il1rl1-/- genotypes. N=4 to 5 per group. (H) Experimental scheme of AAV9 injection in either WT or Il33-receptor deficient (Il1rl1-/-) mice at 7 to 9 days of age, followed by harvest at 12 wks, if the mice lived that long. (I) Survival curves of WT and Il1rl1-/- injected pups with either full-length or cleaved active form versions of the recombinant AAV9 vectors. N=5 to 15 per group. (J) Representative image of Masson's trichrome staining of a heart histological sections from a WT mouse injected with AAV9-Il33-(109-270) cleaved form. Inflammatory infiltrate was observed throughout the heart. (K) Representative heart whole mount from WT or Il1rl1-/- mice injected with AAV9- Il33(109-270). Data are presented as mean ± SD. *p<0.05, **p<0.01, ***p<0.001, ****p<0.0001, ns, p>0.05.

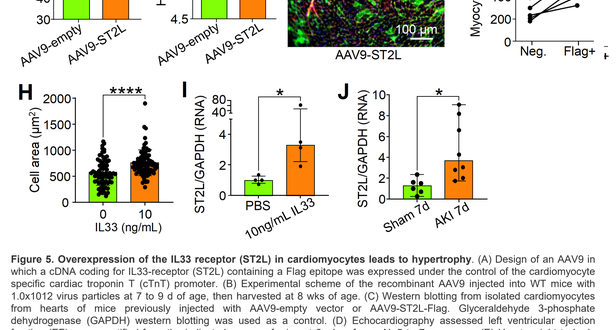

Figure 5. Overexpression of the IL33 receptor (ST2L) in cardiomyocytes leads to hypertrophy. (A) Design of an AAV9 in which a cDNA coding for IL33-receptor (ST2L) containing a Flag epitope was expressed under the control of the cardiomyocyte specific cardiac troponin T (cTnT) promoter. (B) Experimental scheme of the recombinant AAV9 injected into WT mice with 1.0x1012 virus particles at 7 to 9 d of age, then harvested at 8 wks of age. (C) Western blotting from isolated cardiomyocytes from hearts of mice previously injected with AAV9-empty vector or AAV9-ST2L-Flag. Glyceraldehyde 3-phosphate dehydrogenase (GAPDH) western blotting was used as a control. (D) Echocardiography assessed left ventricular ejection fraction (EF) was quantified from the indicated groups of mice at 8 wks of age. N=5 to 7 per group. (E) Heart weight to body weight (HW/BW) ratio in AAV9-CMV-empty vector and AAV9-ST2L-FLAG injected mice at 8 wks of age. N=5 to 7 per group. (F) Representative cardiac histological sections from 8 wk old mice stained for WGA to show cellular outlines and Flag (green) to show the myocytes that were infected with the AAV9-ST2L-Flag construct. Scale bar, 100 µm. (G) Mean myocyte cross-sectional area (µm2) from cardiac histological images as shown in panel F, assessed with ImageJ software for cellular boundaries stained with wheat germ agglutinin (WGA), which were also stained for ST2L expression (Flag+) versus uninfected (Neg) that lacked Flag expression and hence were not expressing ST2L. N=5 and 5 representative histological fields were counted in each heart. Data are presented as mean ± SD (standard deviation). (H) Mean area (µm2) for fixed neonatal rat ventricle cardiomyocytes stained with α-actinin antibody and previously incubated with either 1X PBS or 1X PBS + IL33 10 ng/mL. N=79 and 84 individual myocytes. Data are presented as mean ± SD (standard deviation). (I) RNA expression levels of ST2 in rat neonatal ventricular cardiomyocytes after 1hr in either 1X PBS or 1X PBS + IL33 10 ng/mL Results were normalized with GAPDH RNA expression. N=4 in each group. Data are presented as median ± IR (interquartile range). (J) RNA expression levels of ST2 gene from hearts of wildtype mice subjected to Sham or AKI and harvested 7 days after surgery. Results were normalized with GAPDH RNA. N=6 and 8 respectively. Data are presented as mean ± SD (standard deviation). * p<0.05, **p<0.01, ns, p>0.05.

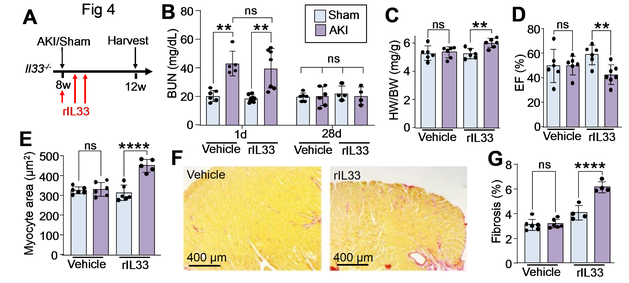

Figure 6. Protection from AKI induced cardiomyopathy in Il33-/- mice is reversed by transient early injection of recombinant Il33. (A) Schematic showing AKI or sham surgery in adult Il33-/- mice injected with either 1 µg of recombinant Il33 (rIl33) or vehicle (sterile 1X PBS), analyzed 4 wks later. (B) Blood urea nitrogen (BUN) levels assayed after 24 hrs and 28 d after sham or AKI surgery in Il33-/- mice injected with vehicle and rIL33. N=4 to 6 per group. (C) Heart weight to body weight (HW/BW) ratio in vehicle and rIL33 injected mice after 28 days of sham or AKI. N=6 per group. (D) Echocardiography measured left ventricular ejection fraction (EF) in Il33-/- mice given vehicle or rIL33, 28 days after sham or AKI. N=6 to 7 per group. (E) Myocyte cross-sectional area (µm2) assessed with ImageJ software on WGA-stained slides from cardiac histological sections in Il33-/- mice given vehicle or rIL33, then assessed 28 days after sham or AKI. N=5 to 6 per group. (F) Representative picrosirius red stained cardiac histological sections from Il33-/- mice given vehicle or rIL33, then harvested 28 days after sham or AKI. Scale bar, 400 µm. (G) Quantitation of the picrosirius red fibrosis staining as shown in panel F, but across 4 to 6 hearts of mice per group, with 5 sections analyzed each. Data are presented as Median ± IR (interquartile range). * p<0.05, **p<0.01, ***p<0.001, ****p<0.0001, ns, p>0.05.

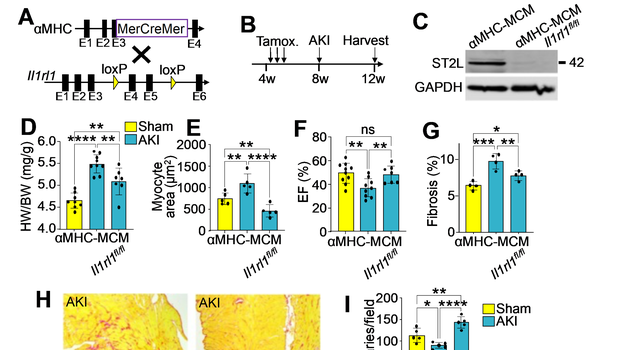

Figure 7. Deletion of the IL33 receptor in cardiomyocytes attenuates AKI-induced cardiomyopathy. (A) Schematic representation of the cardiac-specific αMHC promoter transgene driving expression of the tamoxifen-inducible MerCreMer (MCM) cDNA cassette crossed with a Il1rl1-loxP(fl)-containing gene-targeted allele (Il1rl1fl/fl) for inducible deletion. (B) Experimental schematic of mice receiving tamoxifen to induced cardiac-specific deletion of the loxP-targeted Il1rl1 gene, followed by AKI injury at 8 wks, then harvest and analysis at 12 wks of age. (C) Western blotting to measure levels of ST2L protein in lysates from isolated cardiomyocytes from hearts of αMHC-MCM versus αMHC-MCM;Il1rl1fl/fl mice. GAPDH was used as a loading control. (D) Heart weight to body weight (HW/BW) ratio in αMHC-MCM versus αMHC-MCM;Il1rl1fl/fl mice 28 d after sham or AKI. N=7 to 9 per group. (E) Myocyte cross-sectional area (µm2) assessed in cardiac histological sections with WGA-staining and ImageJ software in hearts of mice 28 d after sham or AKI. N=5 per group. (F) Echocardiography measured left ventricular ejection fraction (EF) in αMHC-MCM versus αMHC-MCM;Il1rl1fl/fl mice 28 d after sham or AKI. N=7 to 10 per group. (G,H) Quantitative evaluation and representative images of cardiac fibrosis in heart histological sections stained with picrosirius red from hearts of αMHC-MCM versus αMHC-MCM;Il1rl1fl/fl mice 28 d after sham or AKI. N=4 per group. Scale bar, 400 µm. N=5 per group for quantitation in G. (I) Quantitation of capillaries per microscopic field (40X objective) with CD31 antibody-based staining of histological images from hearts of αMHC-MCM versus αMHC-MCM;Il1rl1fl/fl mice 28 d after sham or AKI N=5 per group. Data are presented as mean ± SD (standard deviation). * p<0.05, **p<0.01, ***p<0.001, ****p<0.0001, ns, p>0.05.

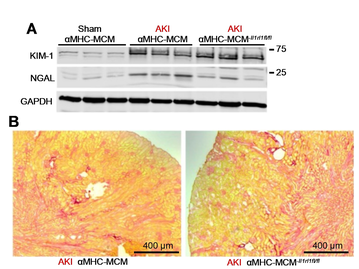

Supplemental Figure 2. Kidney Injury characterization in αMHC-MCM;*Il1rl1*$^{fl/fl}$ and αMHC-MCM mice after AKI. (A) Western blotting for KIM-1 and NGAL (lipocalin-2) in kidney lysates 24 h after sham or AKI in αMHC-MCM;*Il1rl1*$^{fl/fl}$ and αMHC-MCM mice. Glyceraldehyde 3-phophate dehydrogenase (GAPDH) was used as a loading control. **(B)** Representative picrosirius red staining of kidney histological sections 28 d after AKI surgery αMHC-MCM;*Il1rl1*$^{fl/fl}$ and αMHC-MCM mice. Scale bar, 400 µm.